INFLAMMATORY FIBROSIS

M. Ben Amar, *Laboratoire de Physique Statistique, Ecole Normale Supérieure, UPMC Univ Paris 06,24 rue Lhomond, 75005 Paris, France . Téléphone : 01 44 32 34 77 Adresse(s) électronique(s) : benamar@lps.ens.fr*

Institut Universitaire de Cancérologie, Faculté de médecine, Université Pierre et Marie Curie-Paris 6,.75013 Paris, France.

Mots clés : Finite elasticity, fibres, buckling, immune system

1 INTRODUCTION

Fibrosis, the formation of excess fibrous connective tissue, seems to be a common way an organism finds for protection, foreign body reaction, and survival. Put on a solid substrate, a drop containing bacteria (*bacillus subtilis*) (Ben Amar and Wu, 2014) extends by constructing a fibrous gel called biofilm. The fibrous matrix adheres strongly and organizes the cell division. For humans, fibrosis occurs as a reaction of the immune system against aggression : wounds (Martin,1997), solid tumour growth (Stylianopoulos *et al.*, 2012), implants (Moyer and Ehrlich, 2013) and also severe obesity. When it becomes excessive, it induces pathological complications, unaesthetic in the best cases, painful and dangerous for survival in the worse cases. Moreover, the fibrotic tissue, difficult to eliminate physically, limits the transport of drugs, and the preferred solution remains surgery. Fibrosis also occurs around growing tumors. The competition between the immune system cells and the tumor cells is at the origin of the formation of a dense extra-cellular matrix with severe consequences for blood/lymphatic vasculature and drug transport. inside the tumors The course will be devoted to the biophysical and biomechanical study of the growth of a collageneous tissue due to inflammation having in mind both the capsular tissue around breast implants (Moyer and Ehrlich, 2013) and its excessive contracture but also the case of desmo-plastic tumors. For both cases, there exists an immediate wound-healing response with a complex signaling cascade , the final and long-term result being an encapsulation of the implant or the tumor by an inflammatory collagenous tissue.For implants, more easy to study, several causes have been investigated such as bacterial infection, anterior radiotherapy, structure and surface texture of the implant.

I will show a bio-mechanical study including an evaluation of the stresses induced by the growth of the capsular tissue. When it occurs, in the worse cases, the implant is crumpled or fractured, with visible deformity of the breast and pain for the patient. The breast and implant deformations will be explained by a buckling instability inducing a shape bifurcation due to constrained volumetric growth (Ben Amar and Goriely, 2005). To reach this objective, however, requires a good representation of the elasticity of such tissue. Volumetric growth itself generate automatically compressive stresses, increasing during growth and explain the buckling of the samples, the change of shape and perhaps the dolor. Even in the simplest case we can imagine, such as homogeneous volumetric growth of a Neo-Hookean elastic sample, the tissues are submitted to these compressive stresses induced by growth but fibrotic tissues are more complex, stiffer and the prediction of the stresses not obvious.

The stresses may have a double origin : passive or/and active. Passive elasticity for living tissues, or dead elasticity (Thompson,1961) treats living matter as a soft inert material. When the structure evolves with a time scale very long compared to the short time-scale of elasticity (of order the second), the global shape of the sample remains a minimum of the elastic energy. Active means that the sample contains specific cells acting like little compressive motors or point stress sources. Myo-fibroblasts, also originated from the immune system, may play this role, contributing to the pathology. In case of adult wound-healing as an example (Martin, 1997, Wu and Ben Amar, 2014), they are responsible of the final closure of wounds. A good model may help to distinguish between both contributions although we suspect, without precise observations, that these active cells do not exist at the early stages of the pathology. Even remaining at the level of passive elasticity, one needs a correct constitutive law and one part of this work is devoted to this determination by traction tests. We have performed these tests, for the

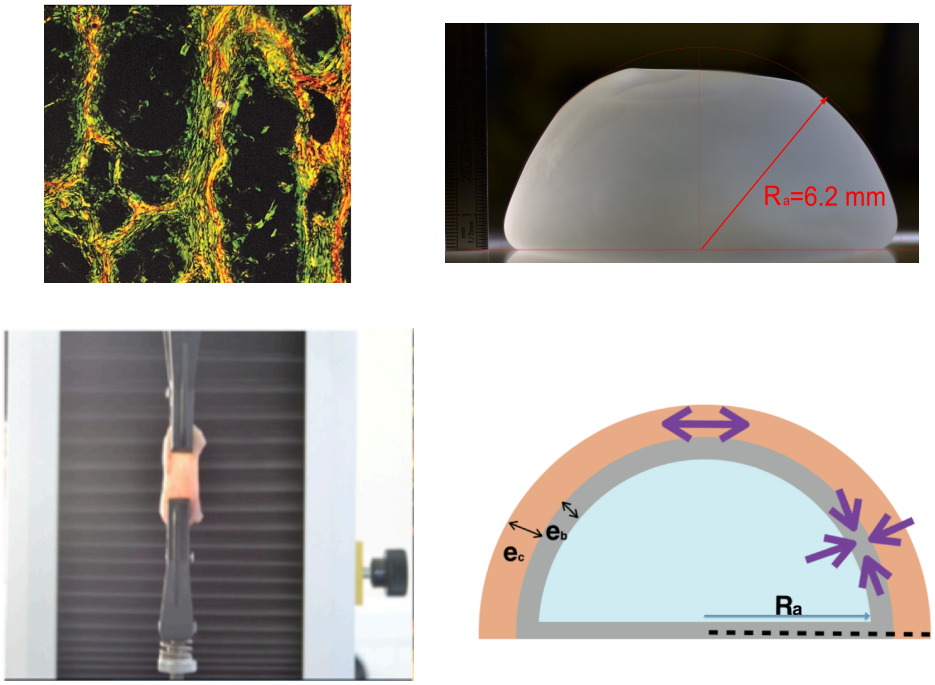

FIGURE 1 – *On top, left- bottom,left*-A schematic example of capsular tissue attached to the traction apparatus. Traction test are performed at constant velocity along the X direction.*On top, right*-Schematic representation of the implant, the capsule and the skin-layer,*bottom, right*-Typical implant for evaluation of the Young modulus using compression and the elastic Hertz contact theory

first time to the best of our knowledge, on surgical tissues obtained post- surgery. Although preliminary, such experimental study is enough to establish a good model of the capsule tissue deformation as a function of its extension.

2 POSITION OF THE PROBLEM, MATERIAL AND METHODS

The peri-prosthetic capsule is a normal physiological response to a foreign object introduced in human body. Soon after surgery, the implanted prosthesis becomes surrounded by an immature tissue made of fibrin mostly and phagocytes. Then collagen and inflammation lead to a mature capsule in 4 weeks approximately. Capsular contracture is the excessive fibrosis around the implant that leads to a high re-operation rate in the lifespan of patients. According to the International Society of Aesthetic and Plastic Surgery, for aesthetic breast augmentation, complication rates are 1% per year, and after 10 years, the rate for capsular contracture exceeds 10% but becomes about 25%, in case of reconstructive surgery after breast cancer treatment. However, rather few publications with histological studies in function of the severity of the pathology are available. According to Moyer and Ehrlich *et al.* (Moyer and Ehrlich *et al.* , 2013) the collagen fibre organization around implant evolves from loosely organization to well spaced thick collagen fibre network when the severity increases (measured by an index or grade) from Baker Grade I up to IV. In addition cells present in light breast capsules like Mast cells seem to disappear for more advanced pathologies. In this case, fibroblasts organize themselves parallel to the fibres or in spiral fashion. The collagen network is cross-linked and more or less parallel to the implant surface. In more advanced stages, muscle-like cells are recruited, contributing to a higher state of stress. A more quantitative study has been published recently, covering capsular contracture cases with all grades. It confirms the increase of the density of the collagen fibres with the grade, the alignment parallel to the surface device (loosely oriented for low Grade, well oriented for contracted capsules) and the presence of myo-fibroblasts for Grade IV capsules (Bui *et al.*,2015). For irradiated patients, the histological damages and changes of the breast skin increases the probability of capsular contracture of high grade.

2.1 Specimen preparation and experimental results

9 biopsies were taken from patients : 5 with Baker III and IV capsular contracture, after implant based reconstruction, and 4 cases concerned breast augmentation for aesthetic purposes (grade I). 2 patients of the first category have previously received irradiation treatment after partial mastectomy. Samples were harvested from surgical specimen of capsulectomy (anterior and posterior). Each sample is cut from the anterior part of the surgical specimen. All the patients have the same brand of implant, the same characteristic of silicone gel and of shell texture (Allergan 410, Anatomical textured implant, texture : biocell). The dimensions of the samples were identical, 1 cm in width, 3 cm in length.The thickness increases with the capsular contraction severity. The specimens were treated in less than two-days (conservation in a sterile saline solution) for tension tests. Once they are excised, the stress due to *in vivo* confined growth is eliminated, but solid stresses or residual stresses may remain in absence of any loading. These stresses are the active part mentioned in the introduction or come from plastic reorganization of the collagen or remodeling during the contracture. The best way to identify such stresses is to cut cuboids carefully and observe the shape as time goes on, make incision and verify the opening, in other words to play with simple shapes immediately post-surgery, then to examine them after few hours.
The deformation of the sample if it occurs after a cut indicates the existence of residual stresses as shown for desmoplastic solid tumors in (Stylianopoulos *et al.*, 2012) for example. An opening indicates a tensile stress and a cusp-like opening indicates a contractile state followed by a tensile one. With such techniques, Stylianopoulos *et al* were able to evaluate the stresses stored during tumour growth of a few kPa with a cartography of their orientation inside the tumor. Another evidence for the presence or absence of residual stresses may be given simply by the behaviour of the uni-axial signal force versus stretch for low loadings. For the set of samples covered by this study no obvious evidence was made of possible residual stresses or of a high density of active cells.
Typical results of the traction experiments performed in the capsular tissues are shown in Figs. (2 A and B), left , that can be compared to equivalent experiment for fabrics. An overview of our experimental measurements indicates that samples can have a positive or negative initial curvature for tensional loading versus stretch, then discontinuities indicating the breakage of fibres by an increase of the tensile force and finally a saturation (see Fig.(2) A and B). To extract informations is made complicated by the inherent diversity of human beings. However, the change of curvature at low stretch seems to be an indication of the degree of the pathology. This change is theoretically examined in details in the next section.

3 DETERMINATION OF CONSTITUTIVE LAWS

3.1 The space of configurations and the stress calculation

We focus here on a cuboid submitted to uniaxial tension along the X axis. We assume that the sample has a length X_0 before stretching larger than the width given initially by Y_0 (in the Y direction) and a thickness Z_0 (in the Z direction). It extends in the X direction, keeping its cuboid shape. This assumption is rather strong but has been checked carefully in our experiment. The surgical cuts are parallel to the implant and correspond to the X, Y plane. We look for simplest solutions taking advantage of the small values of Y_0/X_0 and Z_0/X_0 Then, all stretches defined by x_i/X_i depend only on x, the current configuration coordinate or equivalently on X, the coordinate in the reference configuration before loading. Calling W the hyper-elastic energy, W is a function of the principal stretches : $W(\lambda_1, \lambda_2, \lambda_3)$ with the Cauchy stress given by :

$$t_i = \lambda_i \frac{\partial W}{\partial \lambda_i} - p. \tag{1}$$

λ_i means the principal stretch in the i direction, ratio between the current length l_i of the sample and the initial length L_i, in the same direction. All these quantities λ_i (where the index i takes the value $1, 2, 3$ meaning respectively x, y, z) and p being x dependent. The pressure p is a Lagrange multiplier, which ensures the incompressibility of the sample, giving

$$\lambda_1 \lambda_2 \lambda_3 = 1 \tag{2}$$

In addition because of the mechanical equilibrium, it reads

$$\frac{\partial t_1}{\partial x} = 0. \tag{3}$$

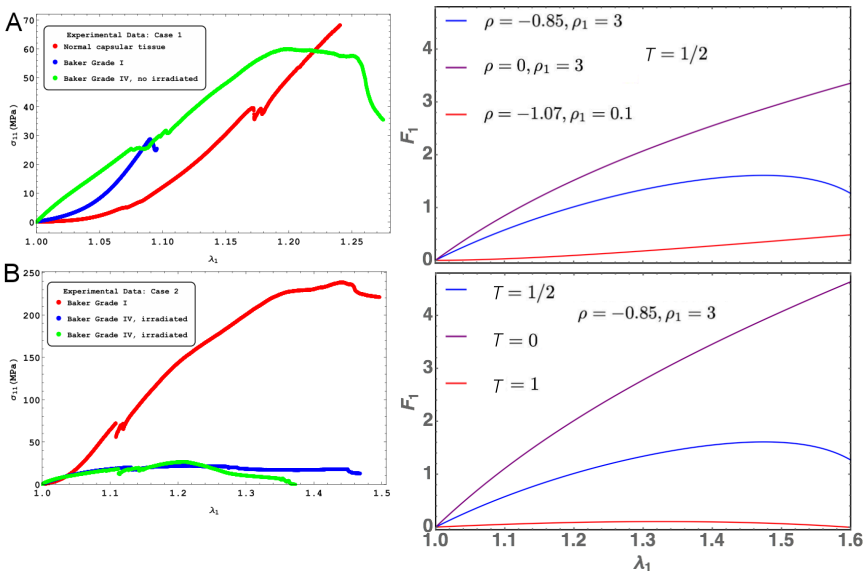

FIGURE 2 – Experimental results : *On left*-A) Experimental stress-stretch relation for different capsular tissues. The orientation of the fibres is unknown. The curves correspond to three different degrees of severity of the fibrosis. The surgery corresponded to a case of breast augmentation for aesthetic purposes. No patient in case A had received a previous irradiation treatment. B) Experimental stress-stretch relation for different capsular tissues. The orientation of the fibres is also unknown. The surgery corresponded to a case of an implant based reconstruction post-cancer. The patient in this case has received an irradiation treatment. *On right* -On top, force versus stretch along the first direction for a sample treated by Mooney-Rivlin biomechanical energy and fully disordered fibres in the C-B mode ($T = 1/2$). The shear modulus is chosen as unit, ρ and ρ_1 varies in order to change the curvature at the origin according to Eq.(12). On bottom, Force versus stretch along the first direction for a sample treated with Mooney-Rivlin bio-mechanical energy and oriented fibres. The shear modulus is chosen as unit, ρ and ρ_1 are fixed to give a priori a negative curvature with $\rho = -0.85$ and $\rho_1 = 3$ but the fibre orientation varies $T = \sin^2\theta_0$.

So t_1 is a constant along x. A similar equation applies for t_2 and t_3 which have also constant values in the sample. Applying now the cancellation of the stress in the Y and Z direction, one gets

$$t_3 = \lambda_3 \frac{\partial W}{\partial \lambda_3} - p = 0 \rightarrow p = \lambda_3 \frac{\partial W}{\partial \lambda_3} \tag{4}$$

Eq.(2) and (4) allow to solve λ_2 and λ_3 as a function of λ_1 to recover the Cauchy stress t_1 as a function of only λ_1. Our experiments determine the uniaxial force :

$$F = \mathcal{A}_0 \lambda_2 \lambda_3 t_1 = \mathcal{A}_0 (\frac{\partial W}{\partial \lambda_1} - p/\lambda_1) \tag{5}$$

with $\mathcal{A}_0 = Y_0 Z_0$. Notice that F is directly proportional to the nominal stress (see the book by Ogden (Ogden, 1984)).
The complete understanding of our experimental results requires a good model for the constitutive law of these tissues with fibres but also a systematic study of these models versus the orientation, dispersion and failure. The experimental analysis including the determination of fibres orientation and dispersion by using optical methods will be considered in a future study. Let us focus in the analysis of our results by using bio-mechanical models which incorporate fibre behaviour at a given orientation and dispersion. Since most of the continuum biomechanics models superpose the elasticity of the ground state to the one of fibres, let us begin by the ground state representation.

3.2 The low stretch biomechanics model

For the ground matrix and applied homogenous strain, restricting on the Mooney-Rivlin model, the energy density for the Mooney-Rivlin model is :

$$W_{MR} = \frac{\mu}{2}\Big\{\lambda_1^2 + \lambda_2^2 + \lambda_3^2 - 3 + \rho(\lambda_1^2\lambda_2^2 + \lambda_2^2\lambda_3^2 + \lambda_3^2\lambda_1^2 - 3)\Big\} \tag{6}$$

where the λ_i, as before, means the principal stretch l_i/L_i. It is possible to replace λ_i by the first invariants I_1 and I_2. The first invariant is I_1 =tr$[\mathbf{F}\mathbf{F}^{\mathbf{T}}]$ while the second I_2 is defined by $I_2 = 1/2(I_1^2 - \text{tr}(\mathbf{F}\mathbf{F}^{\mathbf{T}})^{\mathbf{2}})$ with the deformation gradient being the tensor : $\mathbf{F} = \nabla_{\vec{R}}\vec{r}$. In Eq.(6), μ is called the infinitesimal shear modulus (Ogden, 1984) , having the dimension of a pressure, the Pascal Pa in international units.The Mooney-Rivlin model is an expansion of the elastic energy density limited to I_1 and I_2. To ensure convexity at low strains, the dimensionless parameter ρ can be negative but larger than -1, a restriction which may be revisited for fibrous elasticity.
Fibres (e.g. collagen) are a consequence of the inflammatory process. They may be disordered, polydisperse, cross-linked with arbitrary orientations or with a well defined orientation. They may also contain diverse bundle families. Under stretch, they can reorient themselves in the direction of the stretching or simply break as observed for the fabrics. We suspect that the network more or less stays in the tangent plane of the implant surface. Here the simplest model able to represent our data with the minimal set of independent parameters is taken, knowing that we are faced with fibre remodelling and breakage.

3.3 Mooney-Rivlin and CB fibre model at fixed orientation

Let us begin with the CB model (Ben Amar *et al*, 2015) with fixed orientation θ_0, θ_0 being the angle between the fibres and the stretch direction (X axis). Here I present only a model I have introduced for oriented fibres. To the Mooney-Rivlin ground matrix I introduce an anisotropic contribution :

$$W_{CB} = \frac{\mu_1}{2}\sum_{j=1,2} q_j(\{\mathbf{C}_e + \mathbf{C}_e^{-1} - 2\mathbf{I}) : (\mathbf{E}_j \otimes \mathbf{E}_j)\} \tag{7}$$

where q_j is the material parameter indicating the fibre reinforcements along the direction $\mathbf{E}_j$. For anisotropic materials and an in-plane cross-linked fibre networks, these parameters are a function of the density of fibres times the strength of these fibres in the θ_0 direction. Assuming that the main directions are symmetric with respect to the X axis with equal strength and density, one derives :

$$W_{CB} = \frac{q}{2}\mu_1((\lambda_1^2 + \frac{1}{\lambda_1^2} - 2)\cos^2\theta_0 + (\lambda_2^2 + \frac{1}{\lambda_2^2} - 2)\sin^2\theta_0) \tag{8}$$

with anisotropy only determined by the orientation. This orientation can be dispersed and can remodel with the stretching, inducing a decrease of θ_0. For the lack of knowledge of a preferred orientation, let us choose $\cos^2\theta_0 = \sin^2\theta_0 = 1/2$ which also corresponds to an averaged fibre energy so a fully disorganized fibre network and we find :

$$W_{CB} = \frac{q}{4}\mu_1(\lambda_1^2 + \frac{1}{\lambda_1^2} + \lambda_2^2 + \frac{1}{\lambda_2^2} - 4) \tag{9}$$

which simply modifies the coefficients of the Mooney-Rivlin contribution chosen for the ground matrix, making it stiffer. The elastic density energy is then the sum of both energies as $W_{MR} + W_{CB}$. In this case the calculus of the force can be achieved analytically and gives :

$$\begin{aligned} F = \mu\mathcal{A}_0\Big\{&\lambda_1(1+\rho_1(1-T)) - (\rho+\rho_1(1-T))/\lambda_1^3 \\ &+ \frac{\rho\lambda_1^4(\rho+\rho_1 T) - (1+\rho_1 T)}{\lambda_1^2\sqrt{(\rho\lambda_1^2+\rho_1 T+1)(1+\lambda_1^2(\rho+\rho_1 T))}}\Big\} \end{aligned} \tag{10}$$

with $\rho_1 = q\mu_1/\mu$, (ρ_1 being a dimensionless number characterizing the strength of the fibre network), and $T = \sin^2\theta_0$ which gives to leading order

$$F \sim \mu\mathcal{A}_0\{C_3(\lambda_1 - 1) + C_4(\lambda_1 - 1)^2\} \tag{11}$$

$$\begin{cases} C_3 = \frac{3(\rho+1)^2+4\rho_1(\rho+1)+4\rho_1^2(1-T)T}{1+\rho_1 T+\rho} \\ C_4 = -6(1+\rho+\rho_1(1-T)) + \frac{3}{2}\frac{(\rho+1)(2(1+\rho)+\rho_1 T(3-\rho)}{(1+\rho_1 T+\rho)^2} \end{cases} \tag{12}$$

The model requires, as a necessary but not sufficient condition, C_3 to be positive since it is proportional to the shear modulus. Problems can occur when ρ is negative but only a negative ρ can allow a change in the sign of the curvature (force versus stretch). Since C_3 vanishes for $\rho_\pm = -1 - \frac{2}{3}\rho_1(1 \pm \sqrt{1-3T(1-T)}$, ρ can be negative and smaller than -1, the limit of stability of the Mooney-Rivlin model with fibres. Since we allow remodeling, the sign of C_3 will change also with T, so we must work in a domain of parameters where C_3 is always positive for any value of T, $0 \leq T \leq 1$. However, another limitation comes from the the fact that the force F can diverge. Indeed looking at Eq.(10), a singularity automatically occurs as soon as $\rho = -(\rho_1 T + 1)/\lambda_1^2$ which occurs surely for negative ρ values, when we increase the stretching if the structure of the sample persists. Of course such range of parameters must be eliminated if we remain in this model.

4 EVALUATION OF STRESSES

The capsule is the result of the growth of a thin layer of connective tissue. In case of breast reconstruction, the fat and and gland are eliminated and the implant is covered simply by the nascent capsule and skin. The capsule adheres to the implant, having no possibility to slide or detach. As a result, the growth process is mainly directed along the implant along the normal, making the growth anisotropic and generating automatically compressive stresses. These stresses which appear in the tissue and the implant are called passive. They exist each time when the growth is forced in a direction due to the implant and consists in a particular case of the Biot instability (Biot, 1963). They exist also for an ordinary swelling process of polymeric gel attached on a solid substrate as shown by Tanaka (Tanaka *et al.*, 1987) in pioneering works and among others , for a review see (Dervaux and Ben Amar, 2012). In addition these stresses induced a buckling of the growing layer which distorts the implant. As yet mentioned, the implant has a semi-spherical geometry with a radius of order $R_a = 6.2$ cm. The sphere geometry protects the implant from stresses, however as soon as the sphericity is lost, deformation and stresses occur also in the implant. For completeness we evaluate the Young modulus of our silicone implant by the method of Hertz contact (Landau,1970) (see Fig.(1), on top, right) and obtain 14.7 kPa. Although the theory concerns Hookean elasticity and silicone is mostly Neo-Hookean, we get a good fit . Our stress estimation needs to be compared with shear moduli for the healthy breast fat which varies with the experimental techniques between 2 kPa (Jiang *et al.*, 2015) up to 20 kPa and stiffens in the vicinity of lesions 45.6 kPa for benign one up to 146 kPa for malignant one . All these results have been derived with elasto-sonography *in vivo*. We aim now to evaluate the stresses in the capsular tissues and perhaps to evaluate the active stresses if any. Let us evaluate first the radial deformation due to growth.

4.1 The geometric and elastic deformation tensor

We consider a 3 layered-system in spherical symmetry (see Fig.(1), bottom, left), the implant having the shape of a cap of radius R_a, the capsule occupies the space between R_a and R_b and the thin skin layer the space between R_b and R_c. Because of the presence of the fibres, the growth is assumed anisotropic and the growth tensor reads $\mathbf{F_g} = \text{diag}(g_r, g_r g_\theta, g_r g_\theta)$. g_r represents the relative growth in the radial direction while g_θ is an anisotropic coefficient, identical along meridians and parallels for simplification. The relative volume increase J_G is then given by $J_G = g_r^3 g_\theta^2$. In addition the tissue can be pre-stretched because of active cells and these stretches appear parallel to the implant surface. The pre-stretch tensor which is also a compressive one, $\mathbf{F_{pt}} = \text{diag}(1, \Lambda_\theta, \Lambda_\phi)$, so the deformation gradient becomes $\mathbf{F} = \frac{\partial \mathbf{x}}{\partial \mathbf{X}} = \mathbf{F_e F_g F_{pt}}$ and the elastic tensor is then

$$\mathbf{Fe} = \frac{1}{g_r}\text{diag}(\frac{\partial r}{\partial R}, \frac{1}{\Lambda_\theta g_\theta}\frac{r}{R}, \frac{1}{\Lambda_\phi g_\theta}\frac{r}{R}) \tag{13}$$

Notice that both $\Lambda' s$ are smaller than 1 in case of compressive active stretch which is expected here, as a spontaneous reaction of the immune-system against the implant. The local volume increase is J_G is larger than 1 when the capsule grows. Due to the hypothesis of incompressibility valid for living tissues, also for elastomers, $det\mathbf{F_e} = 1$, so

$$\frac{r^2}{R^2}\frac{\partial r}{\partial R} = J_G \Lambda_\theta \Lambda_\phi = J \tag{14}$$

with $J = 1$ for the implant and also the skin. Focussing only on the determination of the order of magnitude for the stresses involved in the capsule formation, we restrict to a base state of deformation which respects the circular geometry, and we do not treat the full buckling of the capsule with the implant. J represents a control parameter of the buckling process, being a growing function of time if the pathology persists. This full buckling instability is rather technical, some examples can be found in (Ben Amar and Goriely, 2005) for the anisotropic spherical case and in (Wu and Ben Amar, 2014,Wu and Ben Amar) for the cylindrical geometry. The evaluation of the threshold instability given by the critical radial geometric stretch r/R is derived via the solution of an eigenvalue problem involving the control parameters which are, here, the pre-stretch values $\Lambda' s$ and the growth eigenvalues g_r and g_θ. Restricting on the simplest radial solution with an undeformed implant, with the capsule expanding radially, we get the new position of the layers which reads :

$$r(R) = \begin{cases} R & 0 < R < 1 \\ \{JR^3 + (1-J)\}^{1/3} & 1 \leq R \leq R_b \\ \{R^3 + (J-1)(R_b^3 - 1)\}^{1/3} & R_b \leq R \leq R_c \end{cases} \tag{15}$$

where $r(R)$ is the new position of the layer which was initially at a radius R. $r(R)$ respects the continuity at the border zones. Each layer is very thin. In Eq.(15) and in the following, we choose as length unit R_a the radius of the implant.

4.2 Radial Stresses

For simplicity let us assume $\Lambda_\theta = \Lambda_\phi$. In the spherical coordinate system and in the current configuration, the equilibrium equation for the Cauchy stress $\sigma_i = \lambda_i \frac{\partial W}{\partial \lambda_i} - p_i$ (i refers to each layer) gives :

$$r\frac{d(\sigma_{rr}^{(i)})}{dr} + 2(\sigma_{rr}^{(i)} - \sigma_{\theta\theta}^{(i)}) = 0 \tag{16}$$

that we can transform using the elastic stretch $\tau = r/(G_i R)$ into

$$\frac{d\sigma_{rr}^{(i)}}{d\tau} = \frac{A_i}{(A_i - G_i^3 \tau^3)} \hat{W}' \tag{17}$$

with A_i, the coefficient of R^3 into Eq.(15) : $A_i = J$ for the capsule layer and $A_i = 1$ both in the implant and the skin. $G_i = \Lambda_\theta g_\theta g_r$ and $A_i = J$ for the capsule layer while $G_i = 1$ for the implant and the skin. As in (Ben Amar and Goriely,205) and (Ogden,1984), $\hat{W}$ is the elastic energy density for incompressible material $\hat{W} = W(\tau^{-2}, \tau, \tau)$, function of a unique stretch eigenvalue, $\hat{W}'$ being its derivative with respect to the stretch τ. This simplification assumes transversely isotropy. In practice the radius of the implant ($R_a = 6.2$ cm) is larger than the thickness of the layers, of order the millimeter, both for the capsule and the dermis. So the relative thickness e_b of the capsule and e_c the dermis are small dimensionless parameters giving $R_b = 1 + e_b, R_c = 1 + e_b + e_c$ in the reference configuration. To fix the stresses, we begin by the skin and we impose at the outer surface of radius, $\sigma_{rr}|_{R_c} = 0$, corresponding to mechanical equilibrium. So the radial stress inside the skin layer (where no distinction is made between epidermis and dermis) is then given by :

$$\sigma_{rr}^{(skin)} = -\int_\tau^{\tau_c} \frac{1}{1 - \tilde{\tau}^3} \hat{W}'_{skin} d\tilde{\tau} \tag{18}$$

Remember that $\hat{W}'_{skin}$ is scaled by μ_{skin} the shear modulus coefficient of the skin density energy and τ_{skin} is given by

$$\tau_{skin} = (1 + (J-1)(R_b^3 - 1)/R^3)^{1/3} \sim 1 + (J-1)(1-3e)e_b \tag{19}$$

The skin is obviously stretched, however, the stretch differs from 1 inside the skin by a second order coefficient since e is the distance from R_b. So the compression of the skin is given by

$$\sigma_{rr}^{(skin)} \sim \frac{1}{3} \hat{W}'_{skin} Log \frac{(\tau_c - 1)}{(\tau - 1)} \sim \hat{W}'_{skin}(e - e_c) \tag{20}$$

Since e is a dimensionless number corresponding to the radial position $R - R_b$ divided by the implant radius R_a, we recover the Laplace Law where the surface tension γ can be identified as $\hat{W}'_{skin}e/2$ with e given now in international units. For the growing capsule, we have

$$\sigma_{rr}^{cap} = \sigma_{rr}^{skin}|_{R_b} - \int_{\tau}^{\tau_b} \frac{1}{1 - \Lambda_\theta g_\theta \tau^3} \hat{W}'_{cap} d\tau \tag{21}$$

However due to the small thickness of this capsule compared to the initial radius of curvature of the implant, we can estimate the elastic stretch inside the capsule to be :

$$\tau \sim \frac{1}{g_r g_\theta \Lambda_\theta}(1 + (J-1)e) \tag{22}$$

In this limit of small thickness, τ is close to a constant inside the capsule, being given by $\tau_{cap} = 1/(g_r g_\theta \Lambda_\theta)$. It is to be noted that in practice it is difficult to estimate independently these factors and only τ_{cap}^{-1} can be estimated. The radial stress is then

$$\sigma_{rr}^{cap} = \sigma_{rr}^{skin}|_{R_b} + \frac{1}{g_r g_\theta \Lambda_\theta} J\hat{W}'_{cap}|_{\tau=\tau_{cap}}(e - e_b) \tag{23}$$

The capsule remains rather thin except for very pathologic cases, with a thickness which varies from half a millimeter (corresponding to Baker Grade I) to 2 or 3 millimeters (for Baker grade III), which remains small compared to a radius of curvature of order 6 cm, for the implant. Again the radial stress scales as the thickness of the layers. Finally in the implant a radial stress exists at the border given by $\sigma_{rr}^{imp} = \sigma_{rr}^{cap}|_{e=0}$ but our radially symmetric solution does not treat implant deformation. Nevertheless, for a layer size which doubles from grade I to grade III a buckling of the layers occurs as shown in (Ben Amar and Goriely, 2005), the hoop stress being compressive. So now we evaluate this quantity in each layer.

4.3 Evaluation of the order of magnitude for radial and Hoop stresses, layer by layer

In each layer, in radial geometry we have

$$\sigma_{\theta\theta} = \sigma_{\phi\phi} = \sigma_{rr} + \frac{\tau}{2}\hat{W}' \tag{24}$$

For the skin, taking into account Eq.(19, 20), we obtain

$$\sigma_{\theta\theta}^{skin} \sim \hat{W}'_{skin}|_{\tau=1}(e - e_c + \frac{1}{2}) \tag{25}$$

This calculation assumes that there is no proliferation of dermal skin induced by this tensile state which is probably not true. This point will be discussed later. In the capsular tissue, we have

$$\sigma_{\theta\theta}^{cap} = \sigma_{rr}^{skin}|_{R_b} + \tau_{cap}\hat{W}'_{cap}(J(e - e_b) + \frac{1}{2}(1 + e(J-1)) \tag{26}$$

with $\tau_{cap} = (g_r g_\theta \Lambda_\theta)^{-1}$ and $\hat{W}'_{cap}$ being defined for $\tau = \tau_{cap}$ value which is smaller than 1. So the stress is compressive. It is important to notice that the hoop stress is quite independent of the relative thickness of the layer.

4.4 Stresses, buckling and pain

Here, we aim to estimate the mechanical stresses during fibrosis elaboration. Between a capsule of size 0.5 mm, a size we take as initial conditions, to a capsule of 2 mm, the size is multiplied by 4 which is above the stability limit of a spherical layer according (Ben Amar and Goriely, 2005, Ben Amar and Jia, 2013). Indeed the threshold for buckling instability is of order 1.5 for g_r for a stiff substrate and decreases when the substrate is much softer than the layer. We can surely claim that in Grade III, we are above the stability of the spherical symmetry and the whole system will buckle. In addition, our mechanical tests indicate that the tissue itself becomes more and more stiff, the stiffness being

confirmed clinically, being part of the diagnosis. Nevertheless, it is interesting to evaluate the stresses involved which manifest themselves by deforming the breast and implant, explaining the pain and sometimes the rupture of the implant. Let us begin with the skin. It is not so common to find data on the skin, including the dermis, *in vivo*. Here again the thickness involved is of order mm. The Langer lines (Destrade *et al.*, 2013) which give the main orientation of the collagen inside the skin can be assumed along parallels and meridians at the level of the breast. Although we know that the skin elasticity varies a lot along the body, we are not aware of a study of the skin at the level of the breast, for young female beings. In (Destrade *et al.*, 2013), a very precise analysis joining biopsies, traction measurements and modeling have been performed, confirming that the Langer lines of surgeons correspond to the main orientation of the collagen fibres of the dermis and the G-O-H model was shown to correctly represent the skin elasticity in a range of traction identical to our traction test. The structural parameters were evaluated with the coefficients $\mu_{skin} = 0.2014$ MPa, $k_1 = 243.6$ and $k_2 = 0.1327$ while the dispersion coefficient $\kappa = 0.1404$. The skin is stretched by the capsule growth. Keeping the G-O-H model of the skin, we find $\sigma_{\theta\theta}^{skin} \sim \mu_{skin}/4$ so the tension is of order 50 kPa. This number can be over-estimated, however because it assumes no cell proliferation. Being under tension, so under the homeostatic threshold, skin can grow to relax this tensile effect. In the capsular tissue, τ is a quantity which is significantly smaller than 1 and we will choose $1/2$ as a correct estimation. Taking this value we derived $\sigma_{\theta\theta}^{cap} = (1/32)\mu_{cap}(505+126\rho+285\rho_1)$. In the examined cases, we get a compressive stress varying between 7 to 10MPa. This estimation is several orders of magnitude larger than the values of breast fat. It may explain the sensation of stiffness of the capsule, the discomfort and the pain induced by nerve compression.

5 CONCLUSION

Here we present a bio-mechanical study of the contracture of breast capsule at different degrees of the pathology. A tensile test experiment of thin samples obtained few hours post-surgery allows to detect 2 different constitutive laws which may be put in correspondence with the clinical classification. Baker grade I samples seems to present more anisotropy due to well oriented fibres, with breakage of the weakest filaments as the stretch increases. Baker grade III samples are stiffer, however the orientation effect seems to be lost indicating perhaps an increase of the internal disorder. The experiment covers stretch values of order 1.6 corresponding to an elongation of 60%. We test two models of cuboid fibrotic tissues under tension with the difficulty that these models, although common in the literature of biomechanics, exhibit singular behaviour at large strains for some range of the parameters difficult to predict a priori. However an estimate of the parameters corresponding to our results is possible, allowing estimation of the stresses. Our conclusion is that the contracted tissue is extremely stiffer in grade I and III compared to the implant stiffness and to the fat of the breast. This explains the discomfort if the pathological tissue grows as a result of the inflammatory reaction. In addition a buckling instability is expected, beginning at Grade III, leading to distortion of the implant, unaesthetic appearance and sometimes implant rupture, also explained by the ratio between the shear modulus of the implant and the contractile hoop stress of order 3%. Existence of active cells (myo-fibroblasts) can also be suspected at Grade III/IV. However several tests done on the samples with arbitrary cuts as performed in (Stylianopoulos *et al.*, 2012) do not reveal existence of pre-stresses. Pre-stretches are automatically included in the model, while pre-stresses can be introduced. The study of fibrous tissues as a consequence of the immune system and inflammatory response is not limited to the capsular contracture and may be applied to other pathologies such as cancer and severe obesity for example. Future work will concern more advanced critical contractors and the relation between the structure at the microscopic scale and the constitutive elastic laws valid at macroscopic scales.

REFERENCES

Ben Amar M. and Goriely A. 2005 Growth and instability in elastic tissues *Journ. Mech.and Phys. Solids***53** (10), (2005), pp. 2284-2319

Ben Amar M. and Jia F. Anisotropic growth shapes intestinal tissues during embryo-genesis *Proc. Nat. Acad. Sc.*ï£¡**110** (26), (2013) pp. 10525-10530.

Ben Amar, M. Wu, M. Patterns in biofilms : from contour undulations to fold focussing. Eur. Phys. Lett, **108**, (2014), pp. 38003

Ben Amar, M. Wu, M. Trejo, M and Atlan, M Morpho-elasticity of inflammatory fibrosis : the case of capsular contracture. Journ. Roy. Soc. Interface **12**, (2015) 20150343

Biot M.A. Surface instability of rubber in compression *Appl. Sci. Res. A* **12**, (1963),pp.168-182.

Bui JM, Perry T, Ren CD, Nofrey B, Teitelbaum S, Van Epps DE Histological characterization of human breast implant capsules*Aesthetic Plast Surg.***39**(3) :306-315.

Iwahira Y., Nagase T., Nakagami G., Huang L., Ohta Y., Sanada H. Histopathological comparisons of irradiated and non-irradiated breast skin from the same individuals*J Plast Reconstr Aesthet Surg* **65**(11) (2015),pp. 1496-505.

Dervaux J. and Ben Amar M. Buckling condensation in constrained growth *Journ. Mech. Phys. Solids* **59**, (2011), pp.538-560.

Destrade M., Mac Donald B., Murphy J. G. and Saccomandi G.. At least three invariants are necessary to model the mechanical response of incompressible, transversely isotropic materials *Computational Mechanics* 52(4), (2013), pp. 959-969

Jiang Y., Li G-Y., Qian L-X, Hu X-D, Liu D, Liang S.,Cao Y Characterization of the hyperelastic properties of soft tissues using the supersonic shear imaging (SSI) technique :Inverse Method, ex vivo and in vivo experiments, *Med. Image. Anal.* **20** , (2015), pp. 97Ð111. (doi :10.1016/j.media.2014.10.010)

Landau L.D. and Lifshitz,E.M. Theory of Elasticity (Volume 7 of A Course of Theoretical Physics) Pergamon Press (1970)

Martin P. 1997 *Science* **276**, (1997), pp. 75-81

Moyer K.E. and Ehrlich H.P. Capsular Contracture after Breast Reconstruction : Collagen Fiber Orientation and Organization *Breast***131** (4) (2013), pp. 680-685

Ogden R.W. Non-linear elastic deformations Dover Publications and Ellis Horwood (1984)

Stylianopoulos T. *et al* Causes, consequences and remedies for growth-induced solid stress in murine and human tumors *Proc.Nat. Acad. Sc.* **109**, (2012), pp. 15101-15108.

Tanaka T., Sun S.-T.,Hirokawa Y., Katayama S., Kucera J., Hirose Y. and Amiya T. (Mechanical instability of gels at the phase transition *Nature* **325**, (1987), pp. 796-798.

Thompson dï£¡A.W. On Growth and Form. Cambridge : Cambridge University press, (1961)

Wilking J.N., Zaburdaev V., De Volder M., Losick R., Brenner M.P. and Weitz, D.A. Liquid transport facilitated by channels in Bacillus subtilis biofilms *Proc.Nat. Acad. Sc.* **110**,(2013), pp. 848-852.

Wu, M. and Ben Amar M. Growth and remodelling for profound circular wounds in skin *Biomech. Model. Mechanobiol.* **14**, (2015), pp. 357-370.